Electronic supplementary information

Enhanced polysulphide redox reaction using a RuO_2 nanoparticle-decorated mesoporous carbon as functional separator coating for advanced lithium-sulphur batteries

J. Balach,*[a] T. Jaumann,[ab] S. Mühlenhoff,[a] J. Eckert‡[ab] and L. Giebeler[ab]

[a]Leibniz Institute for Solid State and Materials Research (IFW) Dresden e.V., Institute for Complex Materials, Helmholtzstraße 20, D-01069 Dresden, Germany.

[b]Technische Universität Dresden, Institut für Werkstoffwissenschaft, Helmholtzstraße 7, D-01069 Dresden, Germany.

‡ Present address: Erich Schmid Institute of Materials Science, Austrian Academy of Sciences and Department of Materials Physics, Montanuniversität Leoben, Jahnstr. 12, A-8700 Leoben, Austria.

*Corresponding Author

E-mail address: j.balach@ifw-dresden.de

Experimental details

Chemicals

Ruthenium(III) chloride hydrate ($RuCl_3 \cdot nH_2O$), ruthenium(IV) oxide nanoparticles (RuO_2, 99.9 wt%), Ludox HS-40 (40 wt%, 12 nm SiO_2 nanoparticles), elemental sulphur (S, 99.98 wt%), acacia-derived gum arabic (GA), N-methyl-2-pyrrolidone (NMP, 99 wt%), 1,3-dioxolane (DOL, 99.8 wt%, anhydrous) and 1,2-dimethoxyethane (DME, 99.5 wt%, anhydrous) were purchased from Sigma-Aldrich. Super P carbon (SP), lithium bis(trifluoromethylsulfonyl)imide salt ($LiN(CF_3SO_2)_2$, Li-TFSI) polyvinylidene difluoride (PVDF, Solef 21216) and hydrofluoric acid (HF, 40 wt%) as well as lithium nitrate ($LiNO_3$, >99.995 wt%) were purchased from TIMCAL, BASF, Solvay and Merck, respectively. All chemicals were used as received, except Li-TFSI and $LiNO_3$ which were dried at 100 °C under vacuum for 20 h afore.

Synthesis of MPC and RuO_2-MPC composite

The mesoporous carbon (MPC) used as a RuO_2-support material was prepared via SiO_2-templated casting route following our previous report.[1] Here, a resorcinol-formaldehyde polymer was used as a carbon precursor and the weight ratio of SiO_2 to resorcinol was 2.

The RuO_2-MPC composite was synthesised by a facile impregnation-hydrothermal oxidation of $RuCl_3 \cdot nH_2O$ at 200 °C under air, using a modified version of previous works.[2, 3] In a typically procedure, 400 mg of MPC was dispersed in 100 mL of deionized water by ultrasonication for 1 h; then 200 mg of $RuCl_3 \cdot nH_2O$ in 10 ml of deionized water was added to the MPC dispersion. At this point, the pH value of the above mixture was adjusted to 7 using NaOH 0.1 M solution and kept it under vigorous stirring for 15 h. After reaction, the suspension was separated by filtration and repeatedly washed with deionized water, then dried at 80 °C for 20 h and finally heated at 200 °C for 6 h using a heating ramp of 5 °C min^{-1}.

Hybrid separator fabrication

A straightforward modification of the commercially used Celgard polypropylene separator (Celgard 2500) was carried out by casting shaker-milled RuO_2-MPC composite slurry, containing 90 wt% of the composite material and 10 wt% of the PVDF binder in NMP, on one side of the polypropylene separator using the doctor blade method. In a similar procedure, the SP-MPC-coated separator was prepared using a carbon slurry containing MPC, SP and PVDF binder (65:25:10 wt%). The coated separators were dried at 50 °C for 20 h and then cut it into circular disks of 16 mm. The thickness and the added mass of the coatings were, respectively, ≈16 μm and ≈0.3 mg cm^{-2}.

Pure sulphur cathode fabrication

The pure sulphur cathode in this research indicates that the active material is elemental sulphur but not sulphur-based composites. A simple pure sulphur cathode was prepared by shaker-milling elemental sulphur, SP and GA binder[4] (70:20:10 wt%) in deionized water to form a homogeneous mixture and then casting the slurry on an Al current collector by the doctor blade method. The cathode was dried at 60 ºC and 80 ºC for, respectively, 20 h and 2 h and afterwards punched into circular disks of 12 mm. The areal sulphur loading of the cathode is ≈2.0 mg cm^{-2}. In this work, the pure sulphur cathode refers to a simple-designed sulphur cathode prepared with elemental sulphur as the active material instead of a sulphur-carbon composite cathode.[5]

Electrochemical testing

Lithium–sulphur cells were assembled into CR2025 coin-type cells in an Ar-filled glove box with lithium metal foil (Chempur, 13 mm, 250 μm thick) as anode material and reference electrode at the same moment. The electrolyte contains 1 M Li-TFSI and 0.25 M $LiNO_3$ as additive in a 1:1

volume ratio of DOL and DME. Celgard 2500 (16 mm, 25 μm thick) was used as pristine separator. The hybrid separators were placed into the cell with the carbon layer oriented towards the cathode.

Cells were galvanostatically discharged and charged between the potential windows of 1.8–2.6 V at 25 °C using a BaSyTec Cell Test System (CTS). Electrochemical impedance spectroscopy (EIS) measurements were carried out using a VMP3 potentiostat (Bio-Logic) between 200 KHz and 100 mHz using an AC voltage amplitude of 5 mV at the open-circuit voltage of the cells. The cyclic voltammograms were recorded at a scan rate of 0.05 mV s^{-1} between 1.8 and 2.8 V. The combined cycling performance test consists of 10 cycles at a current rate of 0.1 C (1 C = 1672 mA g^{-1}) followed by 90 and 200 cycles at 0.2 and 0.5 C, respectively. The calculation of specific discharging capacities is based on the mass of elemental sulphur while the reported values of the Coulombic efficiency and the degradation rate per cycle are the average values acquired from the corresponding data at 0.2 and 0.5 C (Table S3, ESI†).

Characterisation

A FEI Tecnai F30 transmission electron microscope (TEM) equipped with a field emission gun (FEG) working at 300 kV was used for high-resolution imaging of the mesoporous carbons. The morphology of the RuO_2-MPC and the hybrid separators were examined using a Gemini 1530 scanning electron microscope (SEM) operated at 20 and 5 kV, respectively. Energy-dispersive X-ray spectrometry (EDXS) mapping was used for surface elemental characterisation of the RuO_2-MPC (Bruker EDXS spectrometer). Nitrogen physisorption measurements were carried out at -196 °C using a Quantachrome Quadrasorb SI instrument and the data analysis was performed using the Quantachrome QuadraWin software (Version 5.05). Prior to measurement, the carbon samples were degassed under dynamic vacuum at room temperature for 20 h. The specific surface area was calculated by the multi-point Brunauer–Emmett–Teller (BET) method while the total pore volume

was determined at a relative pressure of $p/p_0 \approx 0.98$. The pore size distribution was obtained using the Quenched Solid Density Functional Theory (QSDFT) equilibrium model. The reported micropore volume is the cumulative pore volume at a diameter of 2 nm obtained from the QSDFT method. X-ray power diffraction (XRD) experiments were carried out in transmission geometry with Cu $K_{\alpha 1}$ radiation on an STOE Stadi P diffractometer with a curved Ge(111) crystal monochromator and a 6°-position sensitive detector. All samples were prepared as thin films on an acetate foil fixed with a collodion glue and were recorded in a 2θ range from 10° to 80° with a step size of $\Delta 2\theta = 0.01°$ with three repetitions. The RuO_2 content in the RuO_2-MPC composite was determined by thermogravimetric analysis (TGA) after combustion in synthetic air at 800 °C (10 °C min^{-1} heating rate) using a Netzsch STA449 Jupiter instrument. Ultraviolet-visible (UV-Vis) absorption spectroscopy was carried out to analyse the relative concentration for the LiPS adsorption of both RuO_2-MPC composite and SP-MPC mixture. The used content of SP in the mixture corresponds to the weight content found for the RuO_2 NPs in the carbon composite, i.e.: 25 wt%. For such purpose, inside an Ar-filled glove box, 4 ml of 0.01 M Li_2S_6 in DOL:DME (1:1 v/v) solution[6] was added to vials containing 10 mg of the carbon samples. The sealed vials were shaken for 4 h and then kept under static conditions for 16 h to decant the carbon material. Then, the supernatant Li_2S_6 solutions were collected, diluted 20 times and analysed by UV-Vis absorption spectroscopy (SPECORD 250 UV-Vis spectrophotometer, Analytik Jena). 0.01 M Li_2S_6 solution was used as a control. The adsorption of RuO_2-MPC composite was normalized to the adsorption of the SP-MPC mixture.

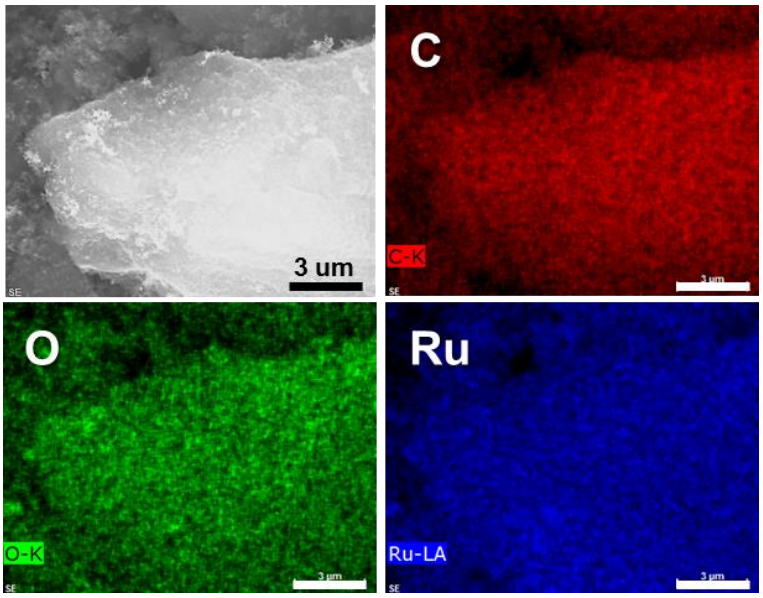

Fig. S1. SEM image and the corresponding EDXS elemental mapping of the obtained RuO_2-MPC composite. Scale bars: 3 μm.

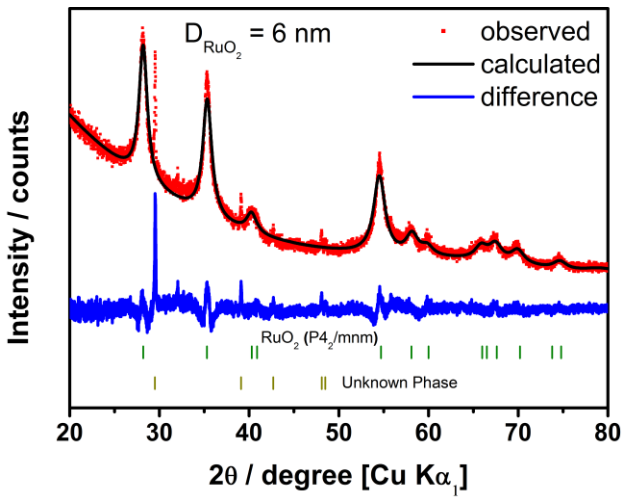

Fig. S2. XRD patterns of the RuO_2-MPC composite.

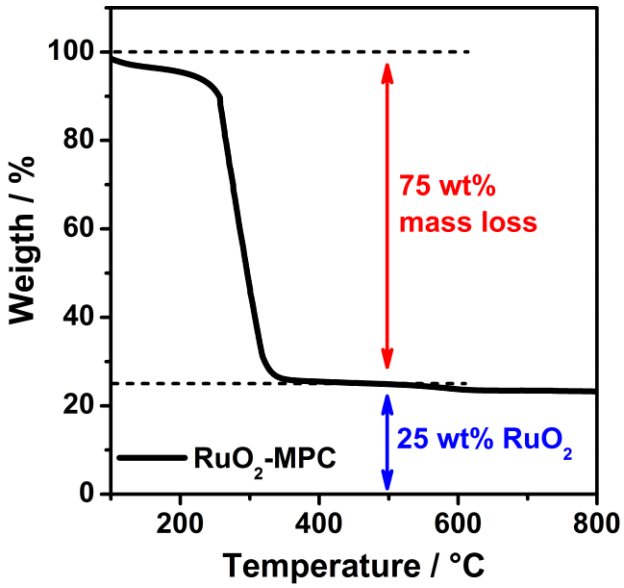

Fig. S3. Thermogravimetric analysis carried out in air-flow of RuO_2-MPC.

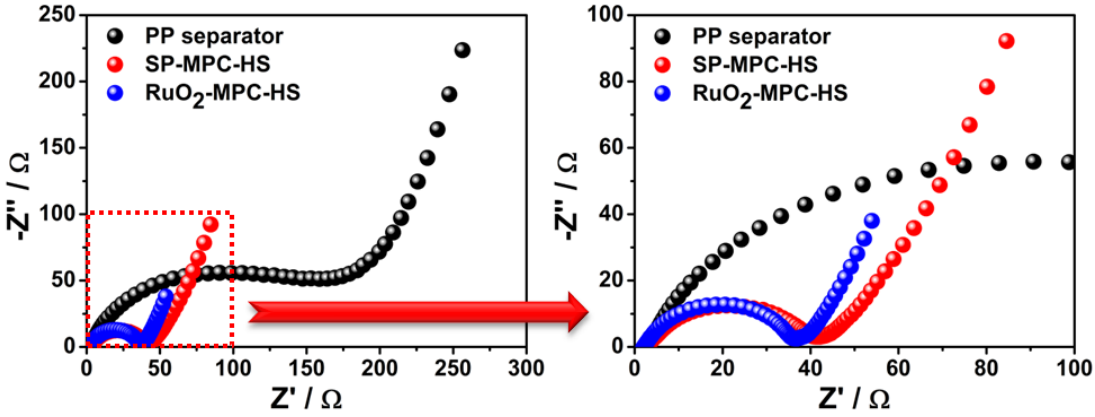

Fig. S4. Nyquist plots of the fresh cells with pristine and hybrid separators.

Table S1. Physical properties of MPC, SP-MPC and RuO_2-MPC materials.

Sample	SSA ($m^2\ g^{-1}$)	S_{micro} ($m^2\ g^{-1}$)	V_{tot} ($cm^3\ g^{-1}$)	PSD (nm)
MPC	728	285	2.23	0.8; 12.2
SP-MPC	695	293	1.92	0.8; 12.4
RuO_2-MPC	543	235	1.69	0.7; 13.9

SSA, specific surface area derived from BET; V_{tot}, total pore volume determined at p p_0^{-1} = 0.98; S_{micro}, micropore surface area determined from the QSDFT method at a diameter of 2 nm; PSD, pore size distribution obtained from the maximum of QSDFT pore size distribution peak.

Table S2. Catalytic parameters of Li–S cells with SP-MPC-HS and RuO_2-MPC-HS obtained from cyclic voltammograms shown in Fig. 4a.

Hybrid separator type	E_I & E_{II}[a] (V)	E_{III} & E_{IV}[a] (V)	I_{II} & I_{III}[b] (mA cm^{-2})	$FWHM_{II}$ & $FWHM_{III}$[c] (mV)
SP-MPC-HS	2.31 & 2.03	2.32 & 2.39	3.44 & 3.00	53.2 & 73.8
RuO_2-MPC-HS	2.32 & 2.04	2.28 & 2.37	4.12 & 3.63	51.1 & 67.4

[a)]redox peak potentials, [b)]current density at the corresponding peak potential and [c)]the full width at half-maximums at the corresponding peak potential.

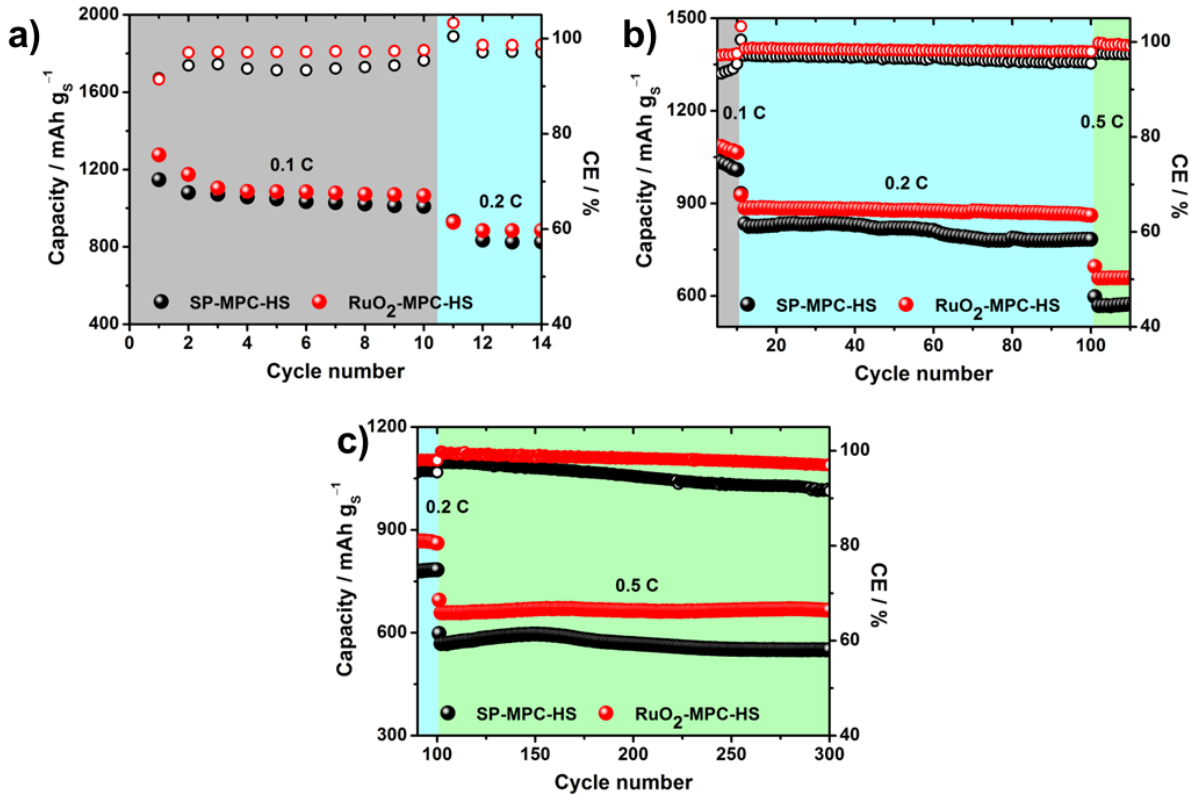

Fig. S5. Combined cycling performance of Li–S cells with SP-MPC-HS and RuO_2-MPC-HS at (a) 0.1 C for 10 cycles, (b) 0.2 C for 90 cycles and (c) 0.5 C for 200 cycles.

Table S3. Comparative cycling stability at each current rate for the Li–S cells with SP-MPC-HS and RuO_2-MPC-HS derived from Fig. S5.

Hybrid separator type	Initial discharge capacity (mAh g^{-1})	Reversible discharge capacity (mAh g^{-1})	Current rate (mAh g^{-1})	Number of cycles	Degradation rate per cycle (%)	CE[a] (%)
SP-MPC-HS	1147	1009	0.1 C	10	1.203	93.9
SP-MPC-HS	932	783	0.2 C	90	0.178	96.5
SP-MPC-HS	598	550	0.5 C	200	0.040	94.5
RuO_2-MPC-HS	1276	1066	0.1 C	10	1.646	96.7
RuO_2-MPC-HS	928	859	0.2 C	90	0.083	98.4
RuO_2-MPC-HS	695	665	0.5 C	200	0.022	98.2

[a)]Average Coulombic efficiency value at the respective current rate.

Hybrid separators modified with a layer of SP/PVDF (SP-HS; 90:10 wt%) and commercial RuO_2 NPs/PVDF ($cRuO_2$-HS; 90:10 wt%) were prepared to highlight the catalytic effect of the RuO_2 NPs on the cycling performance in absence of some porous carbon material with high surface area. The Li–S cell with a $cRuO_2$-HS delivers an initial discharge capacity of 1299 mAh g^{-1} at 0.2 C. After 50 cycles, the cell shows a capacity of 910 mAh g^{-1} and a high CE of 99.4 %. In the case of the SP-HS, the initial discharge capacity, the capacity after 50 cycles and especially the CE are lower than those found for RuO_2-HS (1090 mAh g^{-1}, 652 mAh g^{-1} and 94.2 % respectively). But in terms of costs, the separator modification with only RuO_2 NPs is relative expensive, for this reason it would be more appropriate to use a RuO_2-carbon composite in order to reduce manufacturing costs.

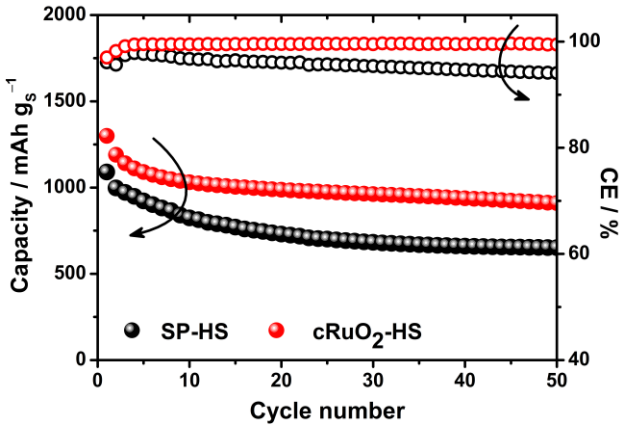

Fig. S6. Cycling performance of the Li–S cells with SP-HS and $cRuO_2$-HS at a current rate of 0.2 C.

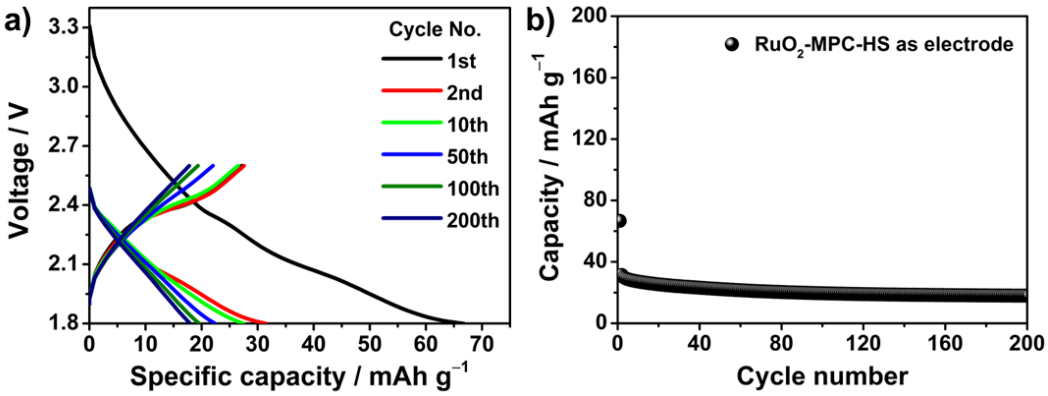

Fig. S7. (a) Voltage profile (1.8–2.8 V) and (b) cycling performance at a current rate of 100 mA g^{-1} for the RuO_2-MPC-HS electrode without sulphur.

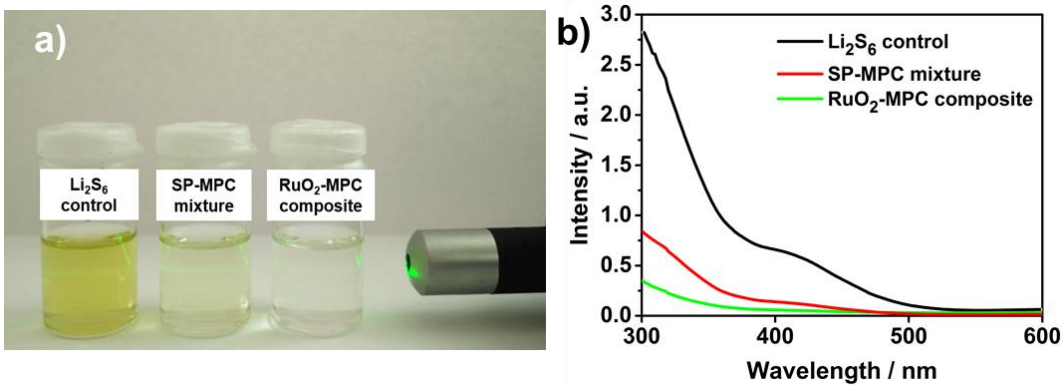

Fig. S8. (a) Photograph of the polysulphide solutions (diluted 20 times with DOL:DME) after adsorption for 20 h and (b) the corresponding UV-Vis absorption spectra. RuO_2-MPC composite and SP-MPC mixture were used as carbon powders for this polysulphide adsorptivity test. Pure Li_2S_6 solution was used for validation purposes. The band around 400−500 nm corresponds to the S_4^{2-} and S_6^{2-} polysulphide species.[7]

References

1. J. Balach, T. Jaumann, M. Klose, S. Oswald, J. Eckert and L. Giebeler, *J. Phys. Chem. C*, 2015, **119**, 4580.
2. R.-R. Bi, X.-L. Wu, F.-F. Cao, L.-Y. Jiang, Y.-G. Guo and L.-J. Wan, *J. Phys. Chem. C*, 2010, **114**, 2448.
3. J. Cruz, V. Baglio, S. Siracusano, V. Antonucci, A. Aricò, R. Ornelas, L. Ortiz-Frade, G. Osorio-Monreal, S. Duron-Torres and L. Arriaga, *Int. J. Electrochem. Sci*, 2011, **6**, 6607.
4. G. Li, M. Ling, Y. Ye, Z. Li, J. Guo, Y. Yao, J. Zhu, Z. Lin and S. Zhang, *Adv. Energy Mater.*, 2015, **5**, 1500878.
5. S.-H. Chung and A. Manthiram, *Adv. Mater.*, 2014, **26**, 7352.
6. J. Balach, T. Jaumann, M. Klose, S. Oswald, J. Eckert and L. Giebeler, *J. Power Sources*, 2016, **303**, 317.
7. Q. Zou and Y.-C. Lu, *J. Phys. Chem. Lett.*, 2016, **7**, 1518.